Visualization of recirculation zones over a perforated plate: An optical flow technique for characterization of fluid dynamics in structured packing

Manasa Iyer, Lionel Vincent, Joel Casalinho, John Pachón-Morales, Mikael Wattiau, Laurent Zimmer, Hervé Duval

Visualization of Recirculation Zones over a Perforated Plate: An Optical Flow Technique for Characterization of Fluid Dynamics in Structured Packing

Manasa Iyer [a], Lionel Vincent[b], Joel Casalinho[b], John Pachón-Morales[a], Mikael Wattiau[a], Laurent Zimmer[c], Hervé Duval[b]

[a] Air Liquide Research and Development, 1 Chemin de la Porte des Loges, Les-Loges-en-Josas 78350, France
[b] LGPM, CentraleSupélec, Université Paris-Saclay, 3 rue Joliot-Curie, 91192 Gif-sur-Yvette, France
[c] EM2C, CNRS, CentraleSupélec, Université Paris-Saclay, 3 rue Joliot-Curie, 91192 Gif-sur-Yvette, France
manasa.periyapattana@airliquide.com; laurent.zimmer@centralesupelec.fr

Abstract. In the context of increasing the performance of structured packing used in distillation columns, we develop a state-of-the-art flow diagnostic method to investigate the intricate fluid dynamics of a falling film interacting with a perforation. Perforations are one of the several key microstructure elements in industrial structured packing whose role in mass transfer enhancement and liquid redistribution is yet not well understood. We focus the present investigation on the liquid curtain, or "twin film", blanketing the perforation. Twin films are prone to strong capillary waves and recirculation zones, and experiments of fundamental nature are required to assess the fluid dynamics in the curtain formation in the perforations and ultimately uncover mechanisms that intensify interfacial mass transfer. Here, a three-dimensional two-component (3D-2C PTV) optical-flow-based technique using the concept of defocus is implemented on a test bench designed to study the effect of perforations on falling liquid films. This method provides an opportunity to evaluate the hydrodynamics of the liquid curtain through streamline patterns and dynamic modes and to describe key features that could promote mass transfer intensification in structured packing.

Keywords Structured Packing, Optical flow, Liquid curtain, Perforations, Flow visualization

1 Introduction

Cryogenic distillation is the leading process for large scale air separation. In this context, distillation columns are usually fitted with structured packing that distribute the liquid phase and promote large exchange area between the rising gas phase and the falling liquid phase. Most structured packing are made of juxtaposed metal sheets that exhibit features such as microtexture, corrugations, or perforations, all of which are recognized to play an important role in the packing performance. However, despite abundant literature on structured packing, the precise role of these features in the flow and distribution of liquid, and ultimately mass transfer efficiency, remain elusive.

Previous work on flow around perforations have shown that these geometric features are associated with profound modifications of the liquid flow on both sides of the plate, most notably by acting simultaneously as obstacles and liquid sinks[1,2]. Moreover, various flow regimes can occur in the perforation: for instance, the liquid may not completely fill the perforation (rim mode), or it may completely cover it (a state known as twin films[3] or liquid curtain[2]). Prior to the transition from the former to the latter, one can observe a wide variety of both permanent and time-dependent phenomena, including the formation of a rim, horseshoe vortices, or the periodic production of drops and columns in the perforation. Twin films, on the other hand, may also exhibit rapid changes in velocity, vortices around all axes, strong variations of thickness profiles and most importantly, unlike supported films, allow phase interaction on both faces of the film.

In real systems, the dense assembly of the packing and the column walls provide little opportunity to observe and access important flow features. Recently, advanced nonintrusive optical techniques such as x-ray[4], gamma-ray[5] tomography, have been implemented to gain insight on the internal flows in packed column. A second approach is to focus on model systems, usually a single sheet including features under study. On such systems it is generally possible to use standard Particle Image Velocimetry (PIV) or Particle Tracking velocimetry (PTV) to unravel complex flow structures in liquid films with time- and spatially-resolved measurements[6].

In this work, we focus on the role of perforations operated in the twin film regime using a fully instrumented model setup mimicking operations conditions of a single packing sheet in a distillation column. Our aim is to gain further insight on the flow phenomena at play in and around the perforations, keeping in mind that the hydrodynamics of liquid curtain may have important implications for the interfacial mass transfer. We implemented an improved 3D2C Particle Image Velocimetry (PIV) optical set-up, which uses the concept of defocus to get access to the depth information. This method was first developed by Baudoin et al[7] in the context of mixing phenomena downstream a spacer grid in a nuclear reactor core. The method is applied here for the first time to falling liquid films.

2 Description of experimental set-up

The experimental setup is shown in figure 1. It consists of a 200 x 150 x 0.5 mm flat aluminium plate punched by a single 4-mm perforation located 60 mm from its top. The plate is held by a rigid frame (ensuring the plate's flatness) and is slightly polished with a fine grit abrasive paper to make the surface less reflective. The flow distribution system feeds the plate on both sides simultaneously with the same flow rate Q. This type of supply system simulates the irrigation system used in industrial structured packings. The liquid circuit and the instrumentation are mounted on a dedicated frame decoupled from the other parts of the system, and the whole assembly rests on an anti-vibration table to damp the parasitic vibrations that may affect the fluid film flowing on the plate

The hydraulic circuit comprises of a flow loop: liquid is circulated from the reservoir to the sample plate and then back to the reservoir through the liquid collector. The liquid from the reservoir circulates thanks to a magnet gear pump (MDG-M15T3B, Iwaki) and deliver the required flow rate to the distributors on each side of the plate. Two flowmeters independently measure the flow rate delivered on each face of the test plate. Needle control valves with the spillway are installed to deliver a constant flow rate at the output.

Experiments were carried out with propan-2-ol (dynamic viscosity $\mu = 0.002$ Pa.s, surface tension $\sigma = 0.021$ N/m) as a working liquid, with an inlet flow rate Q ranging from 16 L.h^{-1} and 42 L.h^{-1}. The choice of the test liquid is done based on the surface wetting properties, mimicking that in cryogenic distillation, in particular liquid nitrogen.

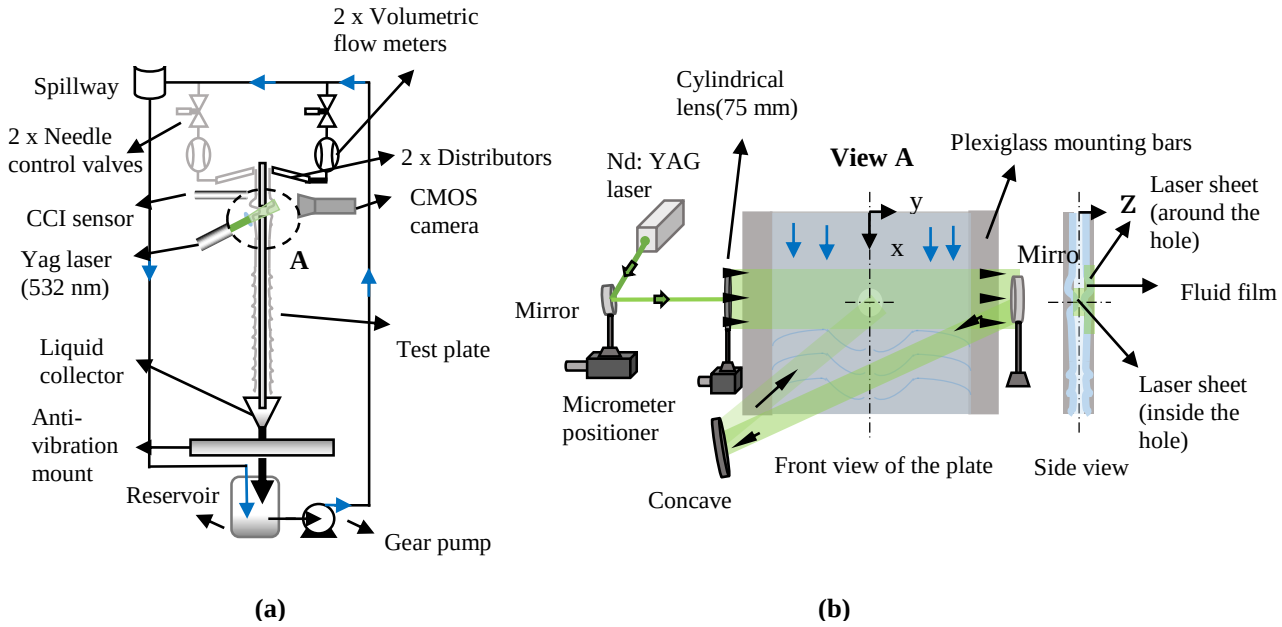

Figure 1 : (a) Experimental setup (one and two face supply configuration). (b) PIV setup with focus on the complex illumination path designed to light both the liquid film and the inside of the perforation.

Optical set-up

The optical part of the setup consists of a CMOS high-speed camera (v310, Phantom) mounted with a macro lens (AF DC-Nikkor 105 mm f/2D, Nikon) equipped with fluorescence filter centered around 570 nm, a Nd-YAG laser (532 nm - 16W - finesse Quantum), optical lenses and mirrors. The continuous laser beam excites the fluorescent tracer particles seeded in the flow. The output power of the laser beam is maintained at a power of 16 W for all the measurements. The laser beam is converted to a laser sheet by a cylindrical lens, which directly illuminate the entire depth of the falling film using a mirror, from the left to right, over the entire width of the plate. The illumination is homogeneous in the zone of measurement in the plate's streamwise (x) and span-wise (y) directions outside the perforation. Special care was needed to ensure the correct illumination of the perforation itself. Indeed, due to the abrupt increase in film thickness around the perforation, the laser sheet insufficiently illuminates the liquid film above the perforation, let alone through it. An additional optical setup was thus implemented to visualize the perforation area, namely a combination of two mirrors and a convex lens with a pre-set tilt angle that refocus the laser beam in the hole.

The flow is seeded with fluorescent tracer particles (480 µL of water suspended fluorescent particles in 2 L of propan-2-ol). The selection criterion for the properties of the particles (diameter (d_p), density (ρ_p)) is based on the Stokes number (St). This number calculates the ratio between the response time of the particles (τ_p) to the Kolmogorov time scale (τ_κ) of the flow.

$$St = \frac{\tau_p}{\tau_\kappa} \; with \; \tau_p = d_p^2 . \frac{\rho_p}{18\,\mu}$$

where ρ_p is the density of the particle, d_p is the diameter of the particle and μ is the dynamic viscosity of the liquid. $St << 1$ signifies that the particle perfectly follows the flow streamlines. For our experiments, a particle size of 20 μm met this criteria and was therefore selected.

All the images are captured with a resolution of 1200×800 pixels at a sample rate of 800 Hz and an exposure time of 1200 µs. A fluorescence filter between the objective and the camera sensor is used to single out the fluorescent tracer particles: specifically, the filter rejects parasite reflections emitted by the aluminium plate and the free surface. The frontal view of the plate is captured by the high-speed camera, which is mounted on a precision positioning platform allowing its orientation to be adjusted in all three directions.

Before each experiment, the test plate is cleaned with a surfactant solution (3 vol% Mucasol, Merz), thoroughly rinsed with distilled water, and dried with compressed air. The parallelism of the test plate with respect to the liquid distributor is carefully adjusted to obtain a liquid film of uniform thickness in the spanwise (y) direction. Then, one or both faces of the plate are first supplied with the highest flow rate (65 L.h^{-1}) ensuring not only that the liquid quickly and entirely wet the full the usable plate width $W = 90$ mm, but also that the liquid completely curtains the perforation and sets the twin film regime. The liquid flow rate is then reduced to the working flow rate, while full wetting and the liquid curtain in the perforation are both maintained thanks to hysteresis[2].

3 Methodology

3.1. Velocity: Optical flow

Images of the particles are processed using an optical flow algorithm approach[8] (see Figure 1). The principle is to determine the intensity displacement (considered an invariant scalar) between two images.

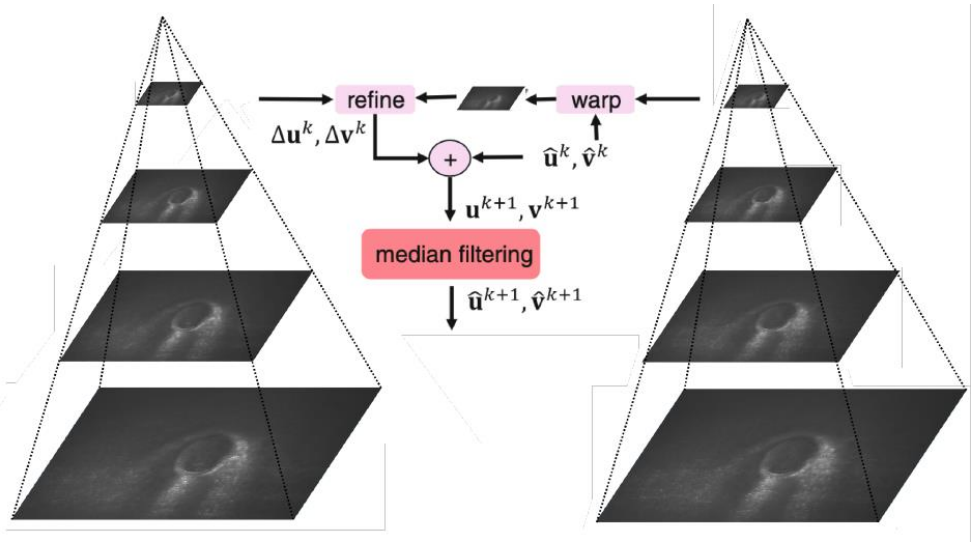

Figure 2 : Optical flow algorithm (u, v are the velocity components in the streamwise and spanwise directions of the plate)

The optical flow method can detect the movement of even a small change in intensity speck of light. The technique can provide a displacement information on each pixel of the image and can thus achieve high spatial resolution. The model uses penalty functions to obtain the optimal velocity vectors. These penalties are generally determined empirically from visual inspection of the acquired images. For the present investigation, we first performed a parametric investigation that showed that optimum parameters were the following: the penalty function is set as the Charbonnier penalty[9] $\sqrt{x^2+\epsilon^2}$ and ϵ is set to 0.0010. Firstly, at each step the unwanted vectors are removed through median filtering, then to further reduce spurious vectors and

uncertainties, a pyramidal approach is used: the method is applied to an under resolved image, then repeated with gradually refined images until the original resolution is reached. Likewise, two time-series data are used to reduce error: typical displacement between image at an instant t and instant $t+1$ is added to the displacement computed between image at an instant $t+1$ and instant $t+2$, and this result is then compared to the displacement measured between image t and image $t+2$.

3.2. Film thickness: Confocal Chromatic Imaging (CCI)

The instantaneous (pointwise) local thickness of the liquid film is measured using a confocal chromatic imaging (CCI) sensor (CL4, STIL). This technique is paramount to measure the thickness of partially transparent films on a flat surface[10]. The sensor can detect multiple interfaces such as solid-liquid, liquid-liquid, and liquid-gas and calculate the thickness between those interfaces making use of the fluid's refraction index. Within the scope of this study, the thickness of liquid film is measured in the supported film area, outside the perforated zone. This device provides pointwise measurements with low error (< 0.5 µm) at a high sampling rate (5000 Hz).

4 Calibration: Liquid film on a flat vertical plate

Preliminary experiments were first conducted on a flat plate as a validation step for the 3D2C method. We performed velocity measurements in the liquid film on an *unperforated* flat plate, otherwise identical to our test plate, under steady flow conditions. We conduct measurements in the liquid film in the same Region of Interest (ROI) where ultimately the perforation is placed. The liquid film is fully developed and uniform along streamwise and spanwise of the plate, as evidenced by pointwise CCI measurements at multiples locations in the ROI (not shown here for brevity).

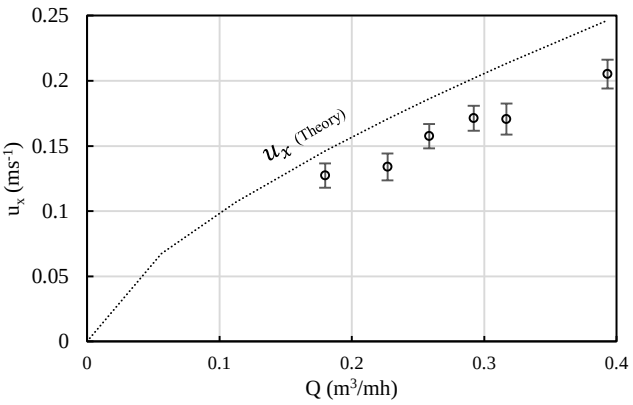

Figure 3 : Experimental mean velocity and theoretical mean velocity for different supply flow rate. Error bars represent the standard deviation for each supply flow condition.

A sequence of raw images sampled at 800 Hz with an exposure time of 1200 µs were pre-processed by enhancing the intensity of fluorescent light emitted by the tracer particles and thus increasing the signal-to-noise ratio of individual particles. We observed stationary tracer particles on the plate at specific regions, and used them as a reference for calibration the depth information. The images were processed with the in-house MATLAB code based on optical flow described in section 3.1. The measurements are repeated for various supply flowrate.

We plot in figure 3 the time- and space-averaged streamwise velocity values for each supply flowrate. This measured mean axial velocity is compared to the theoretical velocity values obtained from Nusselt solution for a flat, developed liquid film. The theoretical value is obtained by integrating the velocity profile within the film thickness ($z = 0\ to\ z\ =\ \delta$), which is assumed to reflect the bulk velocity (see eq. 2).

$$u_x = \frac{g\rho\ sin\theta}{\mu} z\left(\delta - \frac{z}{2}\right) = \frac{g\rho\ sin\theta\ \delta^2}{3\mu} \quad (2)$$

u_x is the streamwise velocity, ρ is the density of the test liquid, μ is the dynamic viscosity of the test liquid, δ is the mean liquid film thickness, and $\theta = 90°$ is the inclination of the plate relative to the horizontal direction. We report that the measured values (circles) are consistently lower than analytical values (dotted line) by approximately 15% for all flow conditions. However, the trend of the measured mean velocity value agrees with that of the theoretical mean velocity.

4. Results

We now present experimental results for a perforated plate irrigated on both sides with equal flow rate, and highlight important flow features in the region of the perforation.

4.1. Visualization of recirculation zones in the suspended liquid curtain in perforation

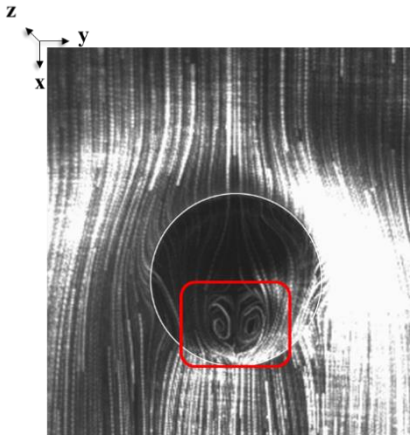

Figure 4 : Streaklines showing the averaged fluid flow in and around the perforation (diameter 4 mm) obtained with 20 superposed high-speed images. Fluid is propan-2-ol, Q = 0.32 m^3/mh.

Figures 4 presents the flow structures in the ROI in and around the perforation operating in curtain mode. The streaklines were obtained by superposing 20 images of the liquid film on a perforated plate, captured at a sampling rate of 800 Hz (exposure time of 1.2 ms). As this image shows, the perforation primarily acts as an obstacle, as evidenced by the outwards deflection of initially vertical streaklines in the upper half. However, unlike the viscous flow around a symmetric body, this flow is not up-down symmetric: the streaklines directly below the perforation are also going outwards and not inwards, while the streamlines immediately adjacent on each side slightly converge, which suggests the presence of a strong pressure gradients and possibly a mixing zone downstream. Now, focusing on the flow inside the liquid film curtaining the perforation, the image clearly shows that the flow is neither uniform nor unidirectional, showing instead quick variations in directions. One characteristic feature stands out: a pair of counter-rotating kidney-shaped vortices (red square) in the lower part of the perforation. We hypothesize that the impingement of the accelerating curtain on the exit edge of the perforation triggers the formation of these vortices.

This feature is present to all tested flow rate and is unique to twin films. Moroever, its presence is of prime importance regarding mass transfer. Indeed, vortices are known to transport the liquid phase toward the interface in counter-current flow, producing steeper concentration gradients at the interfaces, and ultimately promoting mass transfer. Additionally, the bottom stagnation points reduce the liquid film velocity locally, and increase the local residence time and leading to a longer gas-liquid contact time.

4.2. Probability density distribution of velocity vectors

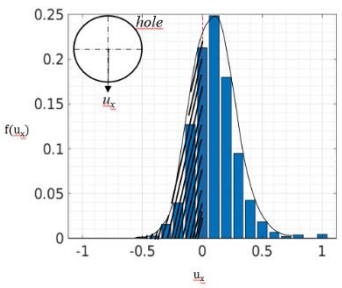

Figure 5 : Probability density distribution of the axial velocity vectors at Q = 0.26 m^3/m.h^{-1}

Taking the quantitative analysis a step further, we now aim to characterize the recirculation zones observed in the film covering the perforation.

Figure 5 shows the probability density distribution of the measured streamwise velocity vectors ($\overrightarrow{u_x}$) strictly contained inside the perforation. We observe both positive (clear area) and negative velocity vectors (hatched area), meaning some fluid particles are going against the flow. However, the intensity of the events with negative velocities is significant (around 40%). These velocity vectors correspond to the particles that move in the reverse flow direction.

Following the same approach, we now examine the probability of negative velocity in the liquid curtain using 2D color maps in the $x - y$ plane. Figure 6 shows this probability maps for two flow rates at each extremity of our operating range: Q = 0.18 m^3/m.h (left) and Q = 0.47 m^3/m.h (right). The color scale ranges from 0 (blue) to 0.5 (yellow), corresponding to 0% to 50%

occurrence of negative velocity vectors. This map allows to quickly locate areas of reverse flow. For the lowest flow rate Q = 0.18 m^3/m (figure 6a), we observe three main region of negative velocities: at the top, center, and at the bottom of the perforation. With increasing supply flowrate, these localized negative velocity regions consistently widen to eventually merge and invade the majority of the perforation area. For Q = 0.47 m^3/m.h (figure 6b) the negative velocity area 60% of the liquid curtain. In the meantime, the streamlines (in black) consistently widen inside the perforation with increasing flow rate, betraying the presence and gradual growth of the recirculation (see section 4.1).

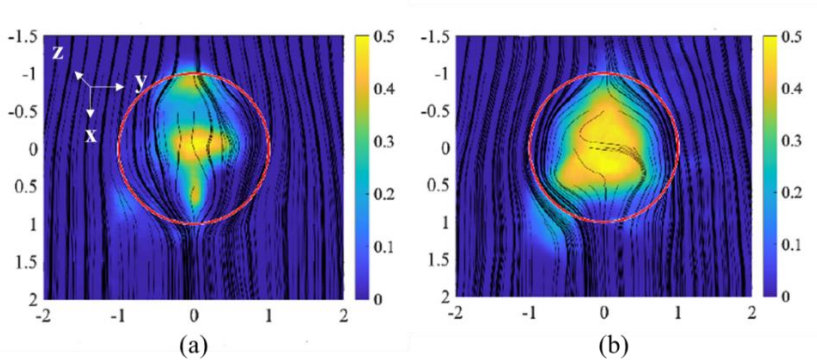

Figure 6 : Probability density map of the negative velocities in and around the perforation ($d = 4$ mm) for (a) Q = 0.18 m^3/m.h and (b) Q = 0.47 m^3/m.h. Two side liquid supply. Black lines are steady streamlines.

4.3. Time-dependent flow characteristics through DMD post processing

In order to characterize the flow dynamics in the liquid curtain, Dynamic Mode Decomposition (DMD) is applied to the time-resolved velocity data. DMD is a mathematical tool widely used to extract the dynamic structures from time-varying datasets.

The post processing method is applied to 3000 velocity field snapshots to extract dominant frequencies. From this analysis, one can extract frequency spectra, such as the one shown in figure 7(a) for Q = 0.18 m^3/mh. A distinct peak, corresponding to the dominant DMD mode, is visible at the frequency 18.16 Hz (signal-to-noise ratio around 1.7). We extract this dominant frequency for all flow rates to obtain the black squares in figure 7(b). We note that the peak frequency identified for each supply condition increases linearly with the supply flow rate.

To confirm these measurements and the origin of this dominant frequency, we performed time-resolved measurements of the liquid film thickness 4 mm upstream of the perforation's upper lip. The measurements were carried out using a CCI probe, at a frequency of 1000 Hz and with an acquisition period of 5s for a more accurate frequency extraction. The signal was then processed using Fast Fourier Transform (FFT) in order to produce a frequency spectrum, from which the dominant frequency of the periodic fluctuations of the thickness was extracted. The resulting frequency for all flow rates is plotted in figure 7(b) in red circles, and shows an almost perfect linearity with Q with a pre-factor of 1.132.

More importantly, the measurements agree very well with the dominant DMD frequency, suggesting that the periodicity of the dynamic structures seen in the perforation is set before the perforation. It is known that periodic fluctuations of measured height in falling films are due to surface (Kapitza) waves[11] travelling down the film, and it may come as little surprise that time-resolved velocity measurements in the perforation pick up the same frequency. However, as we shall see next, the topology of the velocity anomaly suggests that the fluctuations seen in the perforations do not simply reflect the passage of (horizontal) travelling waves, but instead show a perforation-induced asymmetric mode.

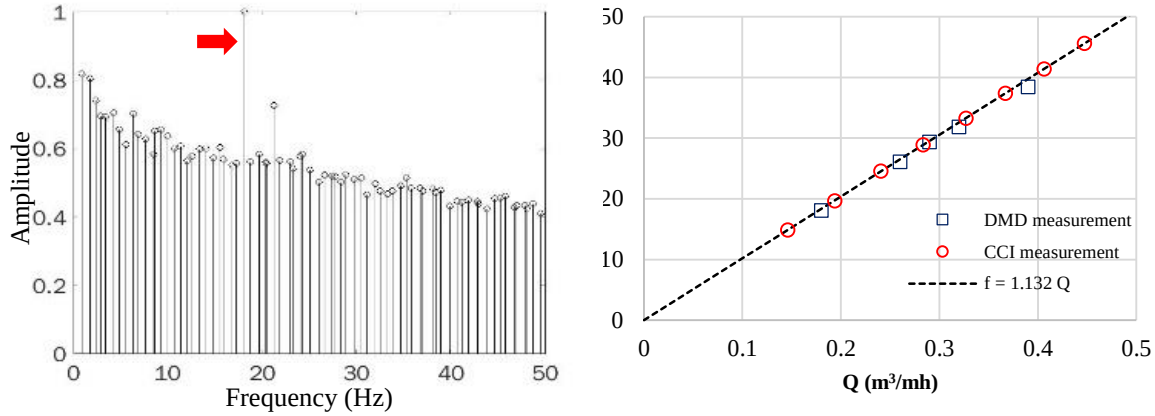

(a) **(b)**

Figure 7 : (a) Frequency spectra obtained from DMD post processing for Q = 0.18 m³/mh. (b) Extracted Dominant frequency for all flow rates.

We pushed the DMD processing a step further and extracted the spatial *modes* associated with the dominant frequency identified in figure 7. In figure 8, we show the typical flow fields associated with those modes, together with the typical vertical velocity (colored). Spatial modes corresponding to the dominant frequencies are reconstructed and plotted at three representative times (phase angles 60°, 120°, 240°) for Q = 0.18 m^3/mh. Red-colored (resp. blue-colored) areas correspond to vertical velocity greater (resp. smaller) than the mean velocity. For the sake of illustration, actual negative axial velocities vectors are added to the positive average velocity. The main feature of this dynamic mode is a streamwise velocity fluctuation mainly affecting the liquid curtain as well as the area just downstream the perforation. This mode is slightly asymmetric; for instance, the bottom-right area never shows neither an excess nor a deficit. The onset of the instability seems to occur close to the perforation entrance.

The spatial modes are characterized by low-frequency fluctuations rather than the expected recirculation observed earlier (see Figure 4). The phenomena of recirculation in twin films is steady and probably the reason we do not capture through DMD.

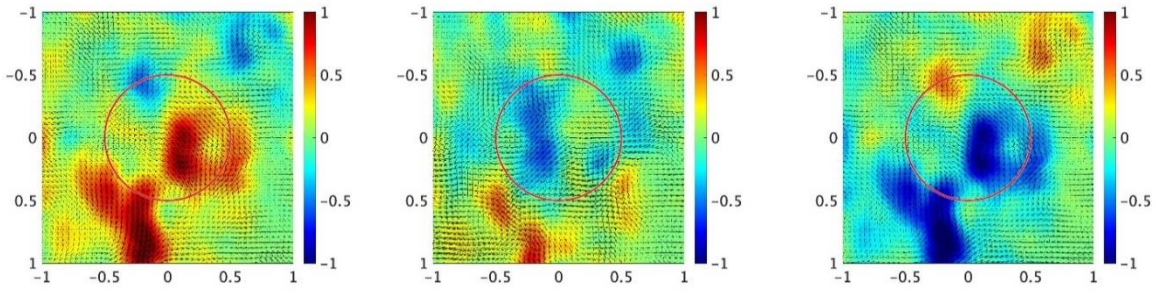

$t \approx 9$ ms ($\phi = 60^0$) $t \approx 18$ ms ($\phi = 120^0$) $t \approx 36$ ms ($\phi = 240^0$)

Figure 8 : DMD spatial mode in the liquid curtain at 18.2 Hz with two-face supply flow rate of Q = 0.18 m³/mh.

5 Conclusions

We present experiments using a novel non-intrusive 3D2C flow diagnostic technique able to resolve the two components of velocity in three dimensions from a single camera using the concept of defocus. This experimental method was implemented for the characterization of liquid film flowing down a vertical perforated plate. A new type of image processing technique using an optical flow algorithm is used to measure velocities in the falling liquid film from the captured images and allows precise probing of the fluid dynamics in and around the perforation.

Local trajectories were measured in the flowing liquid film over and inside a perforation for different supply flow rates. We observed a recirculation in the bottom part liquid film in the vicinity of the bottom stagnation point. We hypothesized that the impingement of the curtain on the exit edge of the perforation results in a pair of counter-rotating vortices (kidney-pair vortices). Those recirculation zones were evidenced quantitatively by negative film velocities, detected in the liquid curtain. These vortices are a unique feature of twin films and could be of a prime

importance regarding mass transfer due to the mixing properties of such vortices, inducing steeper concentration gradients at the interfaces while increasing the local residence time.

Finally, a DMD analysis is applied to extract the dynamic structures of the liquid curtain and allows the reconstruction of spatial modes corresponding to the dominant frequencies of the flow field. The dominant flow patterns in the liquid curtain appear in the form of low frequency, side to side fluctuations. These oscillations are seemingly initiated at the entrance of the perforation, develop in the liquid curtain and propagate downstream the perforation.

The present work is a stepping stone towards a global understanding of the role of macro and microstructures in packing design, and highlight promising features that could be exploited in the search for a better performance. However, follow-up studies involving mass transfer measurement would be necessary to confirm their impact in mass transfer intensification in corrugated and perforated structured packing.

6 Acknowledgements

This research was supported by Air Liquide Research & Development and by Association Nationale de la Recherche et de la Technologie ANRT (CONVENTION CIFRE N° 2017/1472). The authors express their gratitude to Sebastien Gauthier and Frederic Lesage for their technical contribution to the project. The authors acknowledge.

Bibliography

1. Xie H, Hu J, Wang C, Dai G. Liquid flow transition and confined free film formation on a vertical plate with an open window. *Exp Therm Fluid Sci*. 2018;92(July 2017):174-183.

2. Iyer M, Duval H, Casalinho J, Seiwert J, Wattiau M. Experimental study of a liquid film flowing over a perforation. *AIChE J*. 2021;67(11):e17363.

3. Xie H, Hu J, Dai G. Numerical simulation on flow behavior of twin-liquid films over a vertical plate with an open window. *AIChE J*. 2018;64(4):1458-1468.

4. Schug S. Imaging of Fluid Dynamics in a Structured Packing Using X-ray Computed Tomography. 2016;(8):1561-1569.

5. Fourati M, Roig V, Raynal L. Experimental study of liquid spreading in structured packings. *Chem Eng Sci*. 2012;80:1-15.

6. Gerke SJ, Leuner H, Repke J. Experimental Investigation of Local Film Thickness and Velocity Distribution Inside Falling Liquid Films on Corrugated Structured Packings. 2018;69:1-6.

7. Baudoin R, Zimmer L, Muller T. Development and application of a time resolved dual camera 3D PTV technique around obstacles using defocus concept downstream a spacer grid. 2014;(July).

8. Sun D, Roth S, Black MJ. A quantitative analysis of current practices in optical flow estimation and the principles behind them. *Int J Comput Vis*. 2014;106(2):115-137.

9. Bruhn A, Weickert J SCL meets H. Combining local and global optic flow methods. *Int J Comput Vis*. 2005;61(3):211–231.

10. Kofman N, Mergui S, Ruyer-Quil C. Characteristics of solitary waves on a falling liquid film sheared by a turbulent counter-current gas flow. *Int J Multiph Flow*. 2017;95:22-34.

11. S. Kalliadasis, C. Ruyer-Quil, B. Scheid et MGV. *Applied Mathematical Sciences*. Vol 57.; 1973.